

## Supporting Information

### **Controlled Crystal Orientation and Reduced Lattice Distortion with Cystamine Dihydrochloride Spacer for Efficient and Stable 2D/3D Perovskite Solar Cells**

Shunhui Liu,<sup>a</sup> Xueying Wang,<sup>a</sup> Yang Zhong,<sup>\*a</sup> Xiao Luo,<sup>a</sup> Yikun Liu,<sup>a</sup> Binlou Gao,<sup>a</sup> Licheng Tan<sup>\*a,d</sup>, and Yiwang Chen<sup>\*a,b,c,d</sup>

<sup>a</sup> College of Chemistry and Chemical Engineering/Institute of Polymers and Energy Chemistry (IPEC) /Film Energy Chemistry for Jiangxi Provincial Key Laboratory (FEC), Nanchang University, 999 Xuefu Avenue, Nanchang 330031, China

<sup>b</sup> National Engineering Research Center for Carbohydrate Synthesis/Key Lab of Fluorine and Silicon for Energy Materials and Chemistry of Ministry of Education, Jiangxi Normal University, 99 Ziyang Avenue, Nanchang 330022, China

<sup>c</sup> College of Chemistry and Chemical Engineering, Gannan Normal University, Ganzhou 341000, China

<sup>d</sup> Peking University Yangtze Delta Institute of Optoelectronics, Nantong 226010, China

E-mail: tanlicheng@ncu.edu.cn (L. Tan); ywchen@ncu.edu.cn (Y. Chen); 352800220008@email.ncu.edu.cn (Y. Zhong)

## ***Experimental Section***

***Materials and Reagents:*** N, N-dimethylformamide (DMF, 99.8% purity), dimethyl sulfoxide (DMSO, 99.9% purity), acetonitrile (99.8% purity), chlorobenzene (CB, 99.8% purity), 4-tert-butylpyridine (tBP) were purchased from SigmaAldrich and used as received without further purification. Lead iodide (PbI<sub>2</sub>, 99.999%), tin (IV) oxide (SnO<sub>2</sub>, 15% in H<sub>2</sub>O colloidal dispersion liquid) and lithium bis(trifluoromethylsulfonyl) imide (Li-TFSI, >98%) were purchased from Alfa Aesar. Cystamine dihydrochloride (CysCl, 96% purity) was purchased from Merck KGaA. Formamidinium iodide (FAI, 99.8%), methylamine iodide (MAI, 99.5%) and methylamine hydrochloride (MACl, 99.5%) were purchased from Xi'an Yuri Solar Co., Ltd. Lead iodide (PbI<sub>2</sub>, 99.9985% purity) and 2,2',7,7'-Tetrakis [N, N-di(4-methoxyphenyl) amino]-9,9'-spirobifluorene (spiro-OMeTAD, 99% purity) were purchased from Advanced Election Technology Co., Ltd. Indium tin oxide (ITO) (transmission >95%) substrates were purchased from South China Science & Technology Company Limited. Unless specified, all chemicals are employed as received without further modifications after purchase.

***Device Fabrication:*** Indium tin oxide (ITO) glass substrates were cleaned by sequential ultrasonic treatment in detergent, deionized water and isopropyl alcohol for 20 min and then dried with a nitrogen stream. Then the substrates were treated with UV-ozone for 20 min in plasma cleaner. SnO<sub>2</sub> colloidal solution was spin-coated on ITO at 3000 rpm for 30 s, and then annealed at 150 °C for 30 min in air. Then the substrates were treated with UV-ozone for 10 min in plasma cleaner to improve the surface wetting before next step. Perovskite active layers were fabricated by two-step interdiffusion process, where 1.5 M of PbI<sub>2</sub> in DMF:DMSO (v/v 900/100) solvent containing CysCl additive with different concentrations (0.5, 1 and 1.5 mg/mL) was spin-coated onto SnO<sub>2</sub> layer and annealed at 70 °C for 1 min. Then, a solution of FAI: MAI: MACl (90 mg: 6.9 mg: 9 mg in 1 ml IPA) was spin-coated onto the PbI<sub>2</sub> at 2000 rpm for 30 s, and the perovskite precursor film was taken out from the nitrogen glove box to ambient air for thermal annealing at 150 °C for 15 min in humidity

conditions (30-40% humidity). After the substrates cooled to room temperature, the spiro-OMeTAD solution was prepared by adding 72.3 mg spiro-OMeTAD in the solvent (CB 1 mL, 4-tertbutylpyridine 28.8  $\mu$ L, Li-TFSI acetonitrile solution 17.5  $\mu$ L, 520 mg mL<sup>-1</sup>). Finally, a 100 nm Ag anode was deposited by thermal evaporation (rate of 1.0  $\text{\AA}$  s<sup>-1</sup>) using a metal shadow mask. The device area was 0.04 cm<sup>2</sup>. All devices' measurements were carried out in drying cabinet at room temperature.

**Characterizations:** Keithley 2400 was used to characterize the current density-voltage ( $J$ - $V$ ) curves. The currents were measured under 100 mW·cm<sup>-2</sup> simulated AM 1.5 G irradiation (Abet5 Solar Simulator Sun2000). The standard silicon solar cell was corrected from NREL and the currents were detected under the solar simulator (Enli Tech, 100 mW cm<sup>-2</sup>, AM 1.5 G irradiation). The forward scan range is from 0 V to 1.22 V and the reverse scan range is from 1.22 V to 0 V, with 20 mV for each step. The scan rate for the  $J$ - $V$  measurement is 0.2 V/s. Devices were stored and tested in the nitrogen-filled glovebox. Scanning electron microscopy (SEM) was conducted on SU8020 scanning electron microscope operated at an acceleration voltage of 5 kV. Atomic force microscopy (AFM) images were measured by MultiMode 8- HR (Bruker) atomic force microscope. X-ray diffraction (XRD) spectra were carried out by using X-ray diffractometer (Bruker D8Discover 25). The ultraviolet-visible (UV-vis) spectra were characterized on UV-2600 spectrophotometer (Agilent Technologies Inc. Cary 5000 spectrophotometer). The Fourier-transform infrared (FTIR) spectra were conducted on Shimadzu IRAffinity-1S and Thermo Scientific Nicolet iS20. The steady-state photoluminescence (PL) spectra were recorded by fluorescence spectrophotometer (Hitachi F-7000) and time-resolved photoluminescence (TRPL) spectra were recorded by an Edinburgh instruments FLS920 spectrometer (Edinburgh Instruments Ltd.). The PL mapping images were conducted by FastFLIM Q2 (ISS Inc.). X-ray photoelectron spectroscopy (XPS, Thermo Scientific ESCALAB 250Xi) was used for binding energy and element distribution analysis. The water contact angle has been recorded at a Krüss DSA100s drop shape analyzer. External quantum efficiency (EQE) values

were measured under monochromatic illumination (Oriel Cornerstone 260 1/4 m monochromator equipped with an Oriel 70613NS QTH lamp), and the calibration of the incident light was performed using a monocrystalline silicon diode. Electrical impedance spectroscopy (EIS) of the devices was performed in a frequency range from 1 MHz to 10 MHz using Zahner electrochemical workstation at an applied bias equivalent to the open-circuit voltage of the cell under 1 sun illumination.

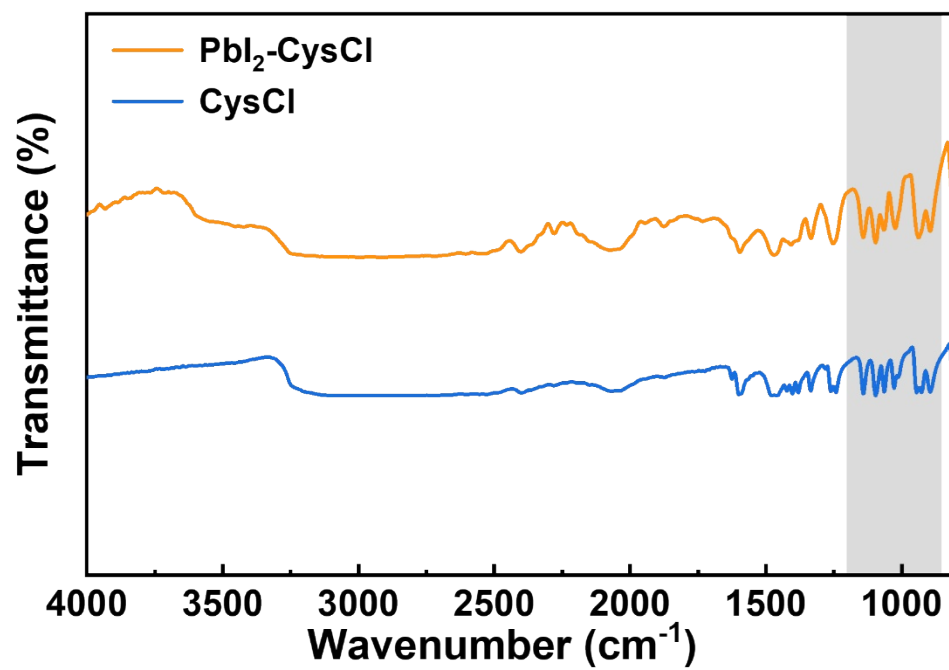


**Fig. S1.** Fourier transform infrared spectrometer (FTIR) spectra of PbI<sub>2</sub> film and PbI<sub>2</sub> film with CysCl.

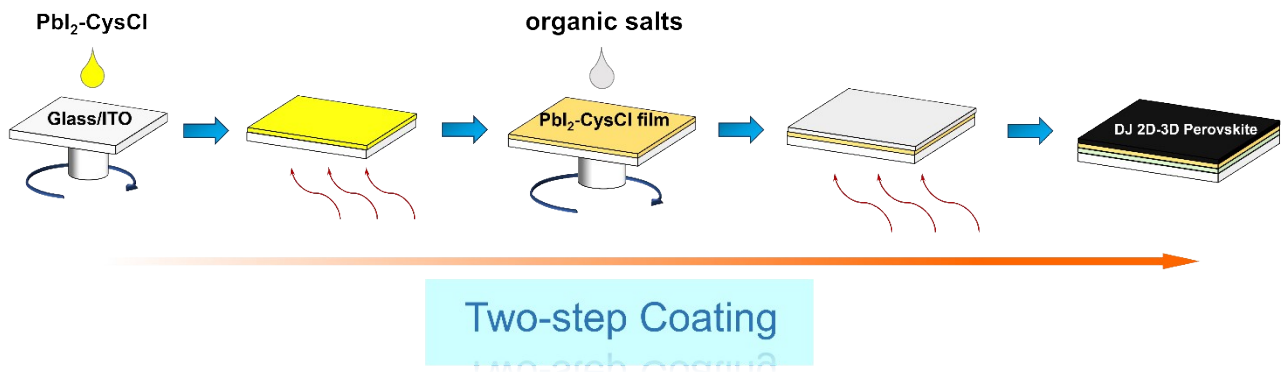


**Fig. S2.** Schematic of preparing 2D/3D perovskite by two-step preparation process.

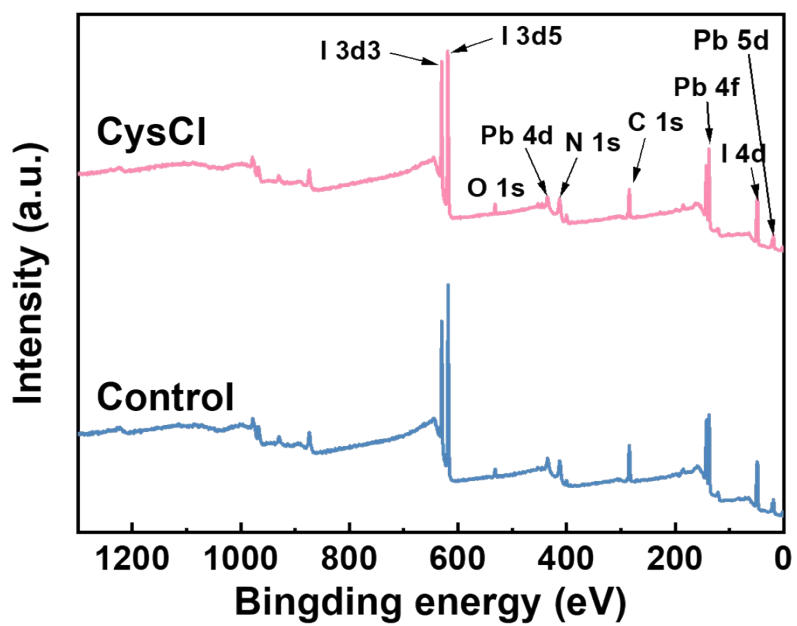


**Fig. S3.** X-ray photoelectron spectroscopy (XPS) of full scan for pure 3D perovskite and 2D/3D perovskite with CysCl.

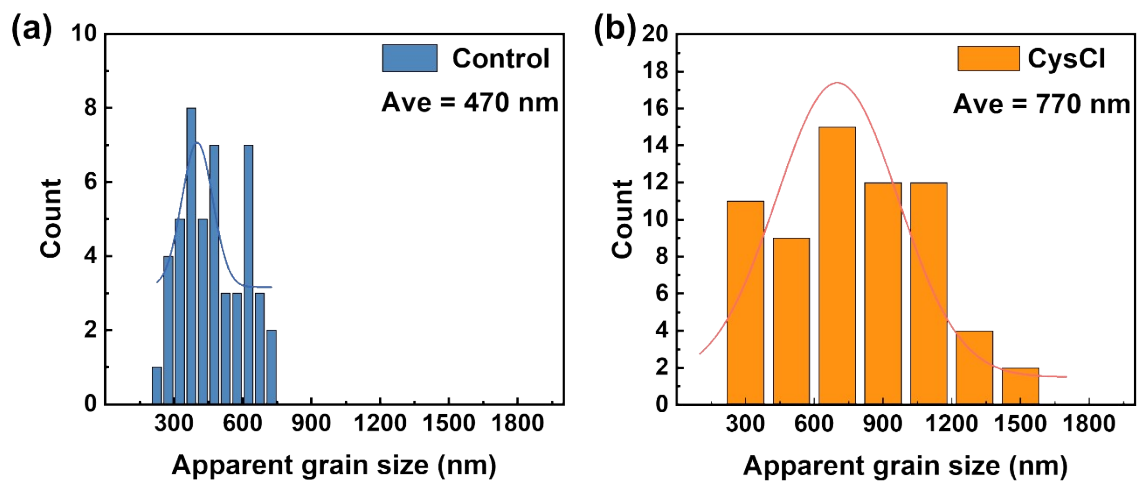


**Fig. S4.** Apparent grain size distributions calculated from top-view SEM images of control and perovskite films with CysCl using the Nanomeasurer 1.2 software.



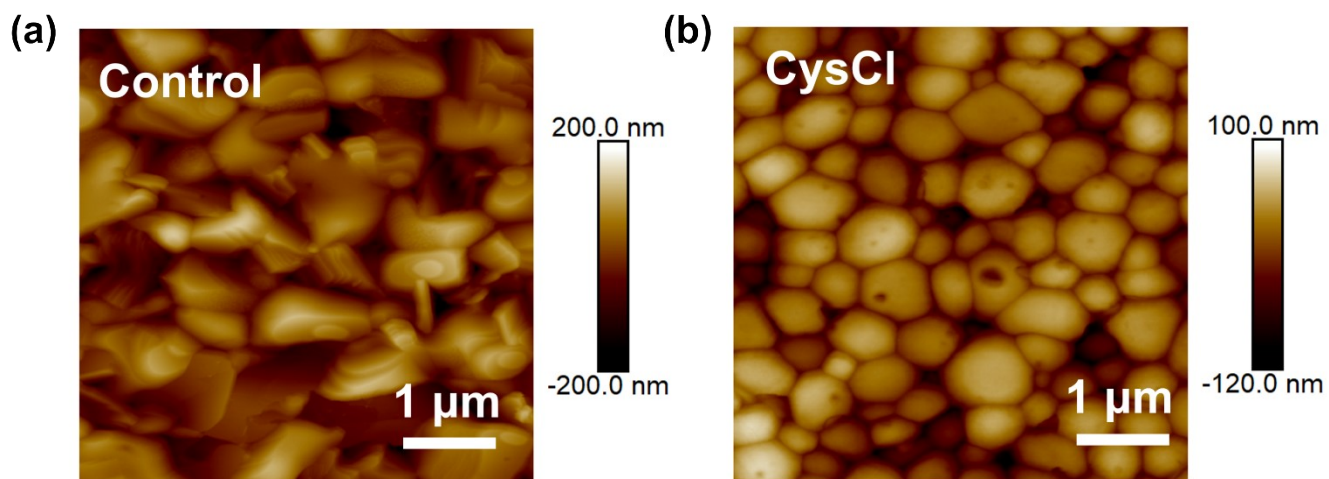


**Fig. S5.** Atomic force microscope (AFM) images of (a) pure 3D perovskite and (b) 2D/3D perovskite with CysCl.

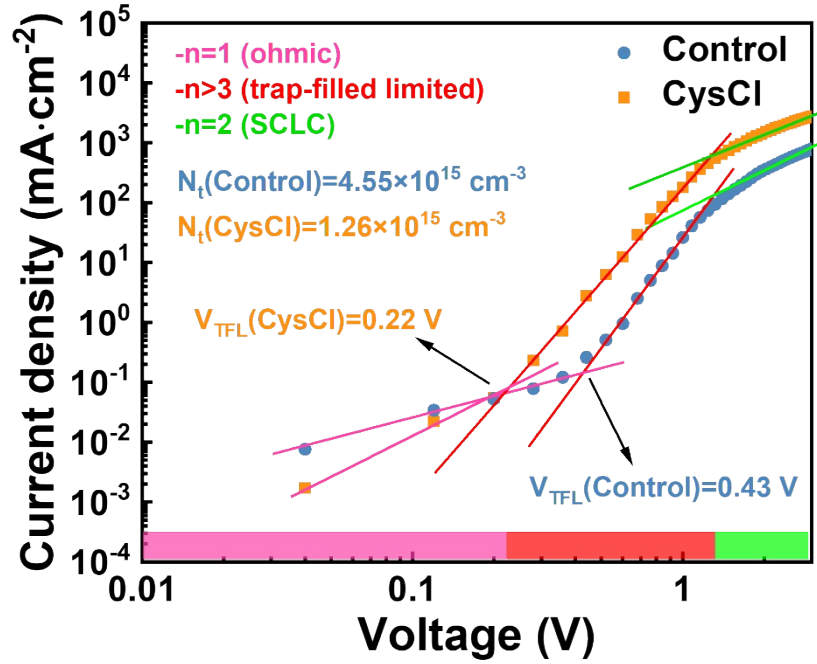


**Figure S6.** Current-voltage ( $J$ - $V$ ) curves for the electron-only devices with structure of ITO/SnO<sub>2</sub>/Perovskite (pure 3D and CysCl-incorporated 2D/3D)/spiro-OMeTAD/Ag based on the space-charge-limited-current (SCLC) model.

The trap density ( $N_t$ ) was calculated using the following formula:

$$N_t = \frac{2\varepsilon_0\varepsilon_r V_{\text{TFL}}}{qL^2}$$

where  $q$  denotes the elementary charge of electron,  $L$  denotes the thickness of the deposited perovskite layer,  $\varepsilon_0$  denotes the vacuum permittivity ( $8.85 \times 10^{-12} \text{ F}\cdot\text{m}^{-1}$ ),  $V_{\text{TFL}}$  is the starting voltage of the trap-filled limit area and  $\varepsilon_r$  denotes the relative dielectric constant (46.9). The calculated trap density ( $N_t$ ) for CysCl-incorporated 2D/3D perovskite is  $1.26 \times 10^{15} \text{ cm}^{-3}$ , which is lower than that of pure 3D perovskite ( $4.55 \times 10^{15} \text{ cm}^{-3}$ ). The results of SCLC demonstrate that the introduction of CysCl can effectively passivate defects.

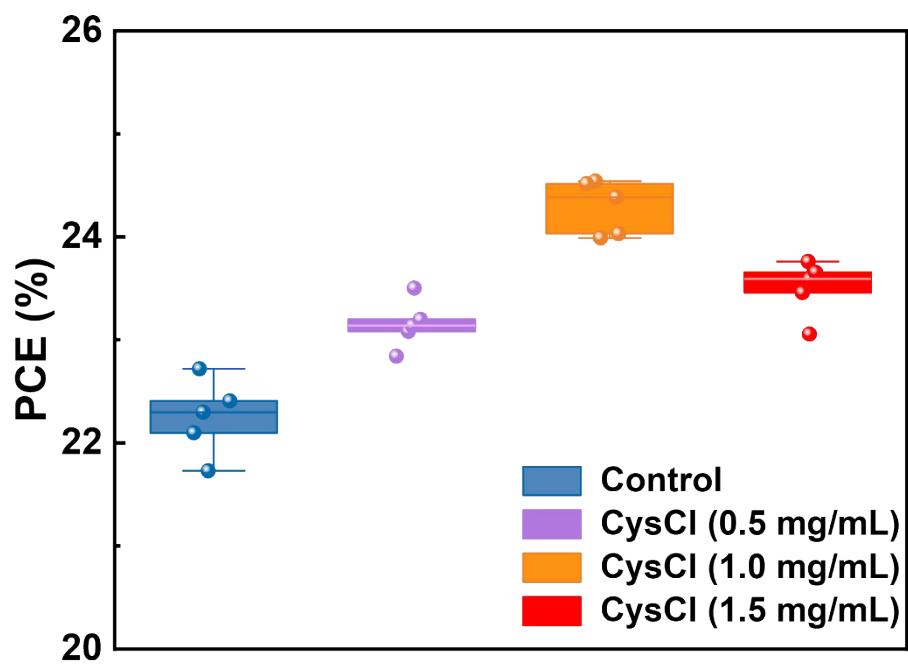


**Figure S7.** Distribution scatter plots of PCE with different concentrations of addition.

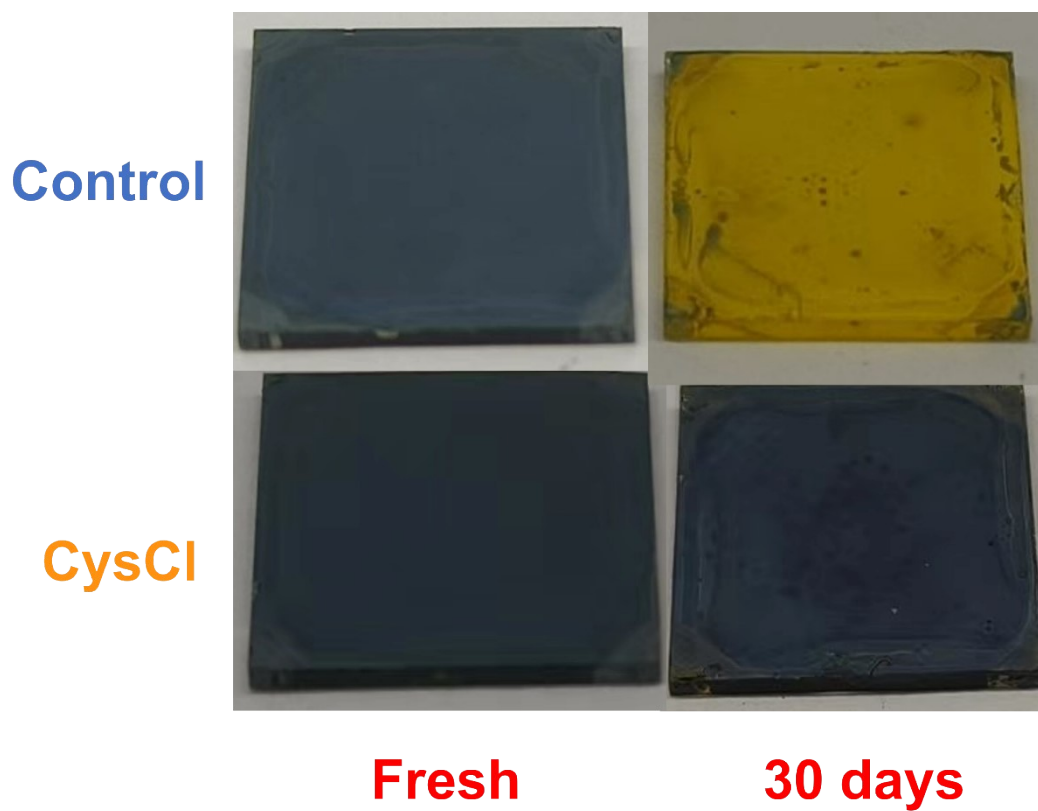


**Fig. S8.** The optical images of pure 3D perovskite and 2D/3D perovskite films with Cyscl upon different exposure durations (fresh and 30 days) in air with  $75\pm 5\%$  RH.

**Table S1.** The parameters of time-resolved photoluminescence measurement of pure 3D and 2D/3D perovskite films with CysCl.

<b>Sample</b>	<b><math>\tau_1</math> (ns)</b>	<b><math>\tau_2</math> (ns)</b>	<b>A</b>	<b>B<sub>1</sub></b>	<b>B<sub>2</sub></b>	<b><math>\tau_{ave}</math> (ns)</b>
<b>Control</b>	61.0	136.1	388.9	3066.7	1432.0	84.9
<b>CysCl</b>	90.8	73.8	104.37	1556.8	5276.7	590.7

**Table S2.** Summary of the simulation parameters for PVSCs based on pure 3D perovskite and 2D/3D perovskite layers with CysCl.

<b>Device</b>	<b><math>R_{ct}</math> (<math>\Omega</math>)</b>	<b><math>R_{rec}</math> (<math>\Omega</math>)</b>
<b>Control</b>	185.6	$1.0 \times 10^4$
<b>CysCl</b>	121.0	$3.0 \times 10^4$